J Wood Sci (2006) 52:44–50
DOI 10.1007/s10086-005-0711-1

ORIGINAL ARTICLE

**Yasushi Nakashima · Masaki Harada · Tomoyuki Hayashi
Masahiko Karube · Tadashi Higashino**

Shear tests of double shear plate connector joints in sugi–Japanese larch composite glulam beams

Received: June 17, 2004 / Accepted: February 21, 2005 / Published online: February 1, 2006

Abstract To study the shear strength of structural joints in sugi (*Cryptomeria japonica* D. Don) – Japanese larch (*Larix kaempferi* Carriere) composite glulam beams using structural connectors with double shear plates, shear tests were conducted on two types of joint (post–beam and girder–beam). Two types of the composite beam (240 and 300 mm depth) were prepared for the tests. Ordinary sugi glulam beam and Japanese larch glulam beam were also used as control specimens. The load–displacement curves of joints in composite beams were somewhere between those of sugi and Japanese larch glulam beams. The shear strength of joints in composite beams was higher than that in the sugi glulam beam control. However, the allowable loads of the joints in composite beams were lower than those in the sugi beam with 240 mm depth. Large variation of maximum load of the joints in the composite beams resulted in lower allowable load.

Key words Sugi–larch composite glulam · Double shear plates · Drift pins · Structural joints · Shear strength

Introduction

Sugi composite glulam beams of which compression and tension laminations are composed of other species with higher strength properties[1] have been proposed to increase the demand of sugi timber. Strength data of these composite glulam beams has been accumulated by several public research organizations to obtain the authorization of the Japanese Agricultural Standard (JAS).[2] However, research on mechanical joints with composite glulam[3] has been sparse.

This study was concerned with the shear strength properties of mechanical joints in sugi–Japanese larch composite glulam beams, using structural steel connectors with double shear plates.

Shear tests were conducted on the specimen using two types of composite glulam beam, and two types of timber joint (post–beam and girder–beam). The strength properties of the joints were compared with those of control specimens using ordinary sugi or Japanese larch glulam beams specified in JAS.

Materials and methods

Specimens

Two types of composite glulam beam were prepared for the test. Figure 1 shows the schematics of the cross section of the glulam beams. The number written in each lamination (e.g., *L*125) is the strength grade specified in JAS. As for the composite glulam beam (hereinafter "composite beam"), the inner laminations were sugi and the outer laminations (two plies for each compression and tension side) were Japanese larch. Ordinary sugi glulam beam (hereinafter "sugi beam") and Japanese larch glulam beam (hereinafter "Japanese larch beam") specified in JAS as *E*65-*F*225 and *E*120-*F*330, respectively, were prepared for control tests. In Fig. 1, *E*65-*F*225 indicates that the average Young's modulus of the products is 65×10^3 kg/cm^2 (6.37 GPa) and the lower 5% exclusion limit is 225 kg/cm^2 (22.1 MPa) at bending strength. The beam depth was 240 mm or 300 mm, and the beam width was 120 mm.

Figure 2 shows the schematics of the structural steel connectors (Kuretec, Tatsumi). Two types of the Kuretec

Y. Nakashima (✉) · T. Higashino
Iwate Prefectural Forestry Technology Center, 560-11 Kemuyama, Yahaba, Iwate 028-3623, Japan
Tel. +81-19-697-1536; Fax +81-19-697-1410
e-mail: y-nakashima@pref.iwate.jp

M. Harada · T. Hayashi · M. Karube
Laboratory of Engineered Wood and Joints, Department of Wood Engineering, Forestry and Forest Products Research Institute, Tsukuba 305-8687, Japan

Part of this article was presented at the 53rd Annual Meeting of the Japan Wood Research Society, Fukuoka, March 2003

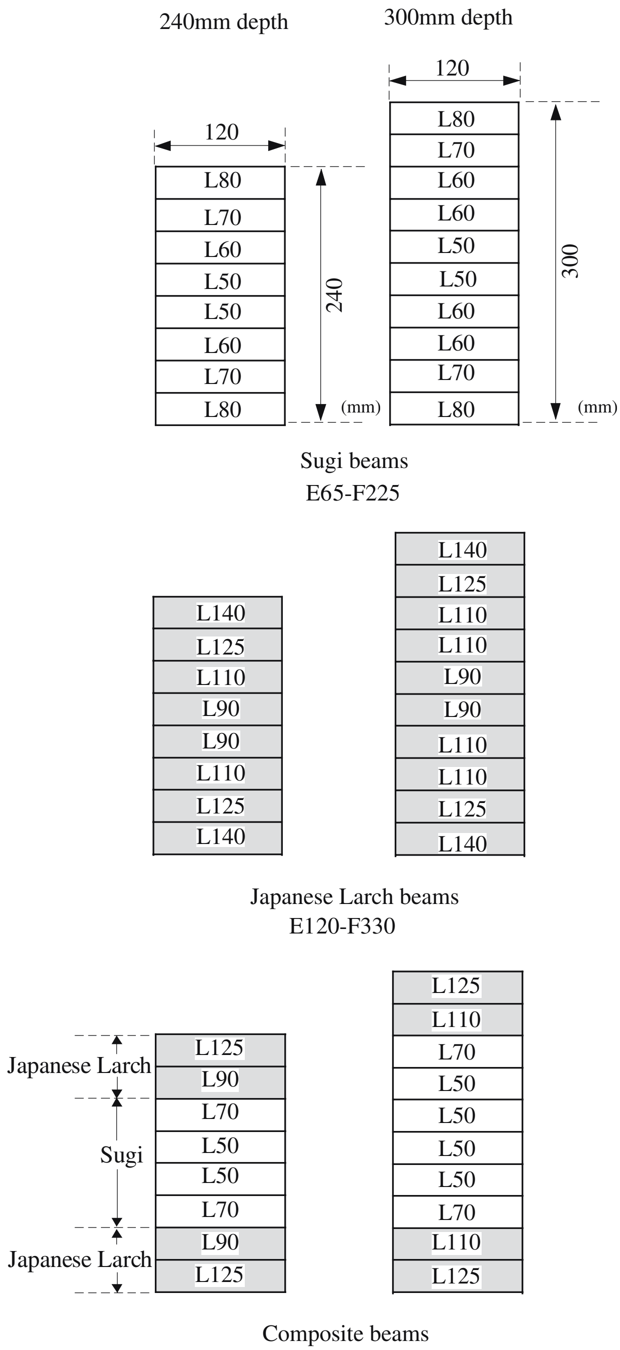

Fig. 1. Cross section of sugi glulam beams, Japanese larch glulam beams, and composite glulam beams

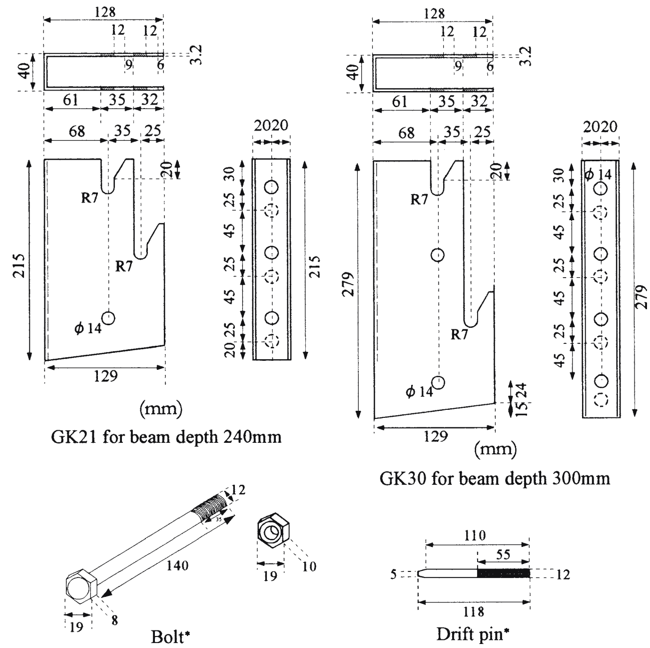

Fig. 2. Geometry of Kuretec connectors. Bolt and drift pin: carbon steel classified 4.6, nominal tensile strength 400 N/mm², lower yield point 240 N/mm²

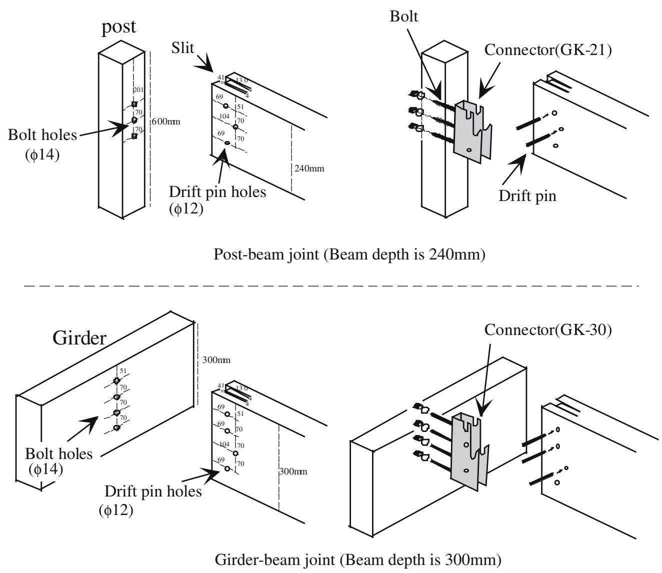

Fig. 3. Joint assembly

connector were used; GK21 was used for 240 mm depth beam, and GK30 was used for 300 mm depth beam.

Kuretec connectors have been widely used in Japan, because general users can use them without obtaining permission for the construction. A main characteristic of the connector is the simple shape with double shear plates, which can be produced easily without any weld or cast. In addition, there is no steel bottom angle or connecting bolt that is used in other structural connectors.[3]

Figure 3 shows the joint assembly in which a beam connects to a post or girder. The joint contains drift pins and bolts. For the post member, sugi glulam composed of homogeneous grade lamination (*L*50) were used. For the girder member, the same glulam as the glulam beam was used. Figures 4 and 5 shows two types of joint: a beam connects to a girder (Fig. 4), and a beam connects to a post (Fig. 5).

Three specimens were prepared for one testing condition. Consequently, 36 specimens (3 types of beam × 2 beam depths × 2 types of joint × 3 specimens) were used for the test.

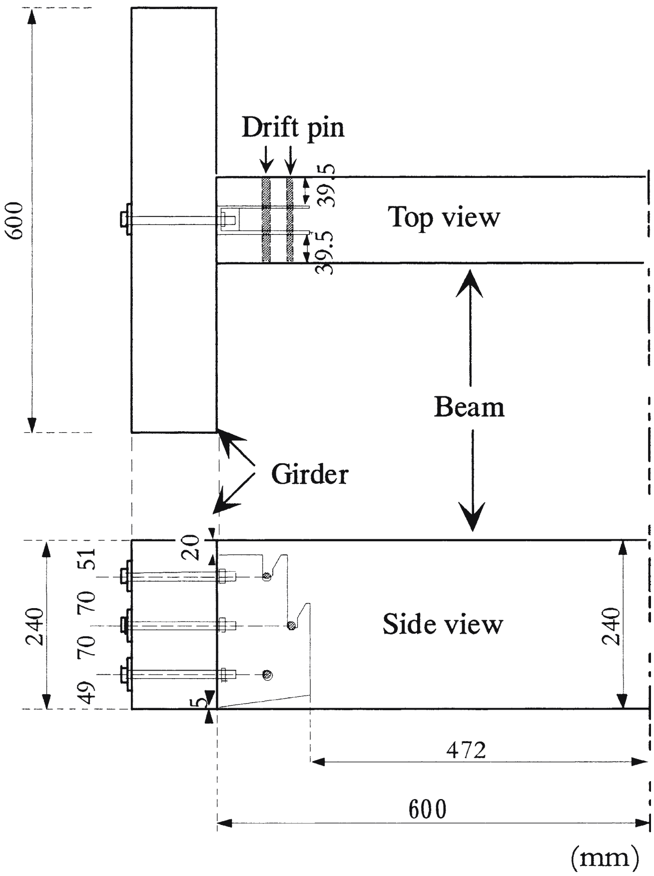

Fig. 4. Girder–beam joint with GK21 connector (240 mm beam depth)

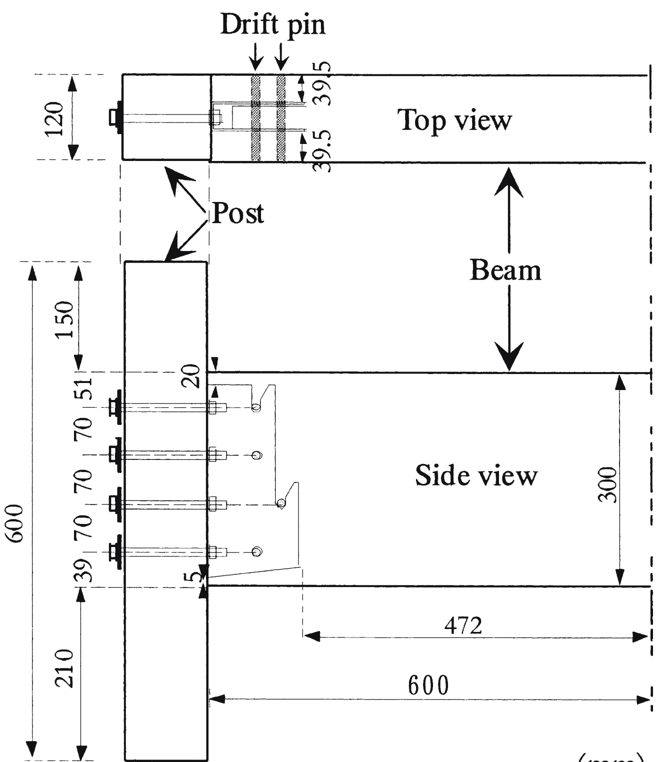

Fig. 5. Post–beam joint with GK30 connector (300 mm beam depth)

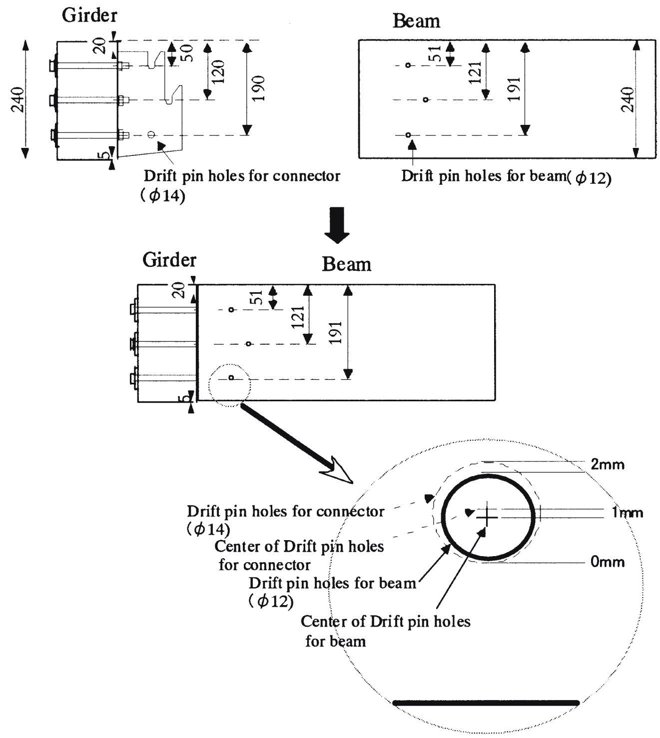

Fig. 6. Clearance of connector and beam

Figure 6 shows the clearance between the connector and beam. The diameter of drift pin holes in the connector is 14 mm. On the other hand, the diameter of drift pin holes in the beam is 12 mm. The distance from the upper edge of the girder to the center of the holes in the connector was 50 mm, 120 mm, or 190 mm. Nevertheless, the distance from the upper edge of the girder to the center of the holes in the beam was 51 mm, 121 mm, or 191 mm. This offset is effective for tightening gaps between the connector and the beam when the drift pins are driven.

Test methods

A hydraulic loading machine with a capacity of 1000 kN was used for the test. Figure 7 shows the schematics of a loading apparatus and a specimen composed of a beam and two posts. Load was applied monotonously to the specimen with two loading heads. Loading was stopped after the load attained a maximum load and then dropped to less than 80% of the maximum load.

During the loading, corresponding values of load and relative displacements were measured. The interval from the beginning of loading to the end was about 7–14 min for each specimen. After the loading test, a small wood block was cut from the specimen, and its moisture content was measured. The moisture contents of all specimens were 13%.

Figure 8 shows definitions and a method for calculating the strength properties of mechanical timber joints. The Japan Housing and Wood Technology Center[4]

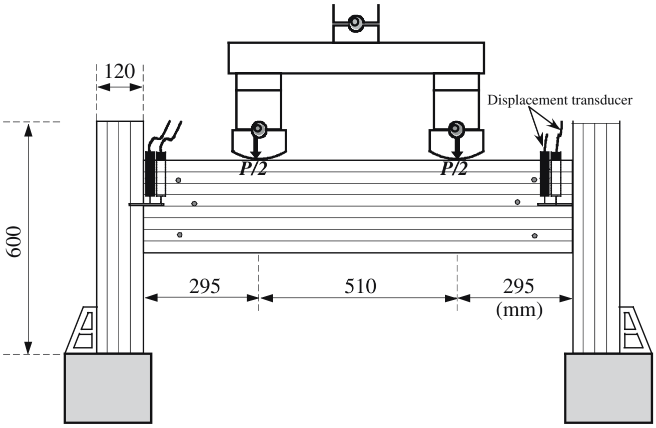

Fig. 7. Loading apparatus and specimen (post–beam joint)

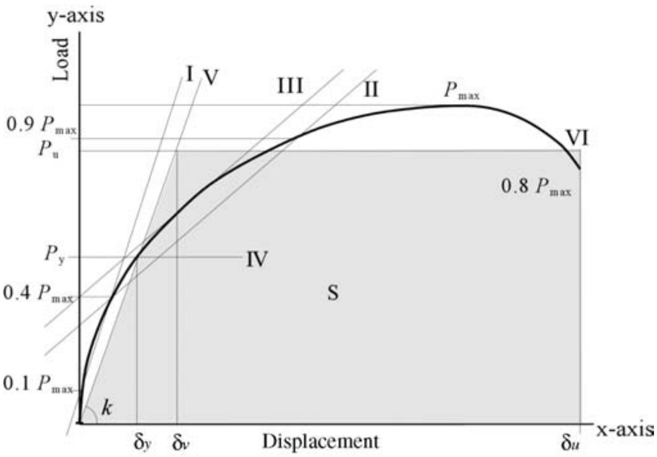

Fig. 8. Definitions for calculating structural characterization factors. P_{max}, Maximum load; k, initial stiffness; P_y, yield strength; δ_y, yield deformation corresponding to P_y; δ_u, maximum displacement; P_u, yield strength to limit; δ_v, yield displacement to limit

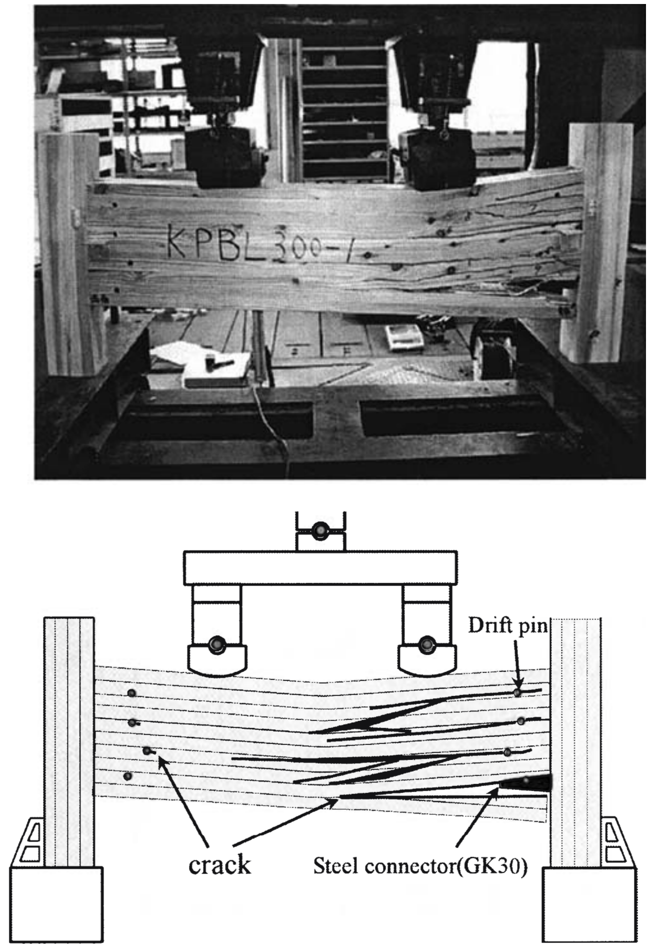

Fig. 9. Typical failure mode of joint

proposed this method, and the calculation is performed as follows:

1. Line I, joining 0.1 P_{max} and 0.4 P_{max} in the load – displacement (L–D) curve is drawn.
2. Line II, joining 0.4 P_{max} and 0.9 P_{max} in the curve, is drawn.
3. Line II is translated along with the x-axis to be a tangent to the curve. This new line is defined as line III.
4. The load corresponding to the intersection of lines I and III is defined as the yield strength (P_y). Line IV is drawn parallel to the x-axis through this point.
5. Displacement corresponding to the intersection of line IV and the curve is defined as yield displacement (δ_y).
6. Line V is drawn joining the origin and the coordinates P_y and δ_y. The gradient of this line is defined as the initial stiffness (k).
7. Displacement at 0.8 P_{max} in the L–D curve after the peak is defined as the maximum displacement (δ_u).
8. The area enclosed by the L–D curve, the x-axis, and δ_u is defined as S.
9. Line VI is drawn parallel to the x-axis so that the trapezoid area enclosed by the x-axis, line V, and δ_u is equal to S.
10. The load corresponding to the intersection of lines V and VI is defined as the yield strength to limit (P_u).
11. Displacement at P_u in the L–D curve is defined as the yield displacement to limit (δ_v).

Allowable load is evaluated by taking the lower value of the following two values: average of $P_y \times$ variation coefficient, or average of maximum load (P_{max}) × 2/3 × variation coefficient, where variation coefficient is $1 - CV \times K$; CV is the coefficient of variation and K is a constant (3.152).

Results and discussion

Failure mode

Figure 9 is an example of the specimen failure showing several splits along the laminations. Cracks initiated at drift pin holes and then progressed as the applied load increased. Other failure modes such as tearing of bolt heads[3] were not observed in any specimens.

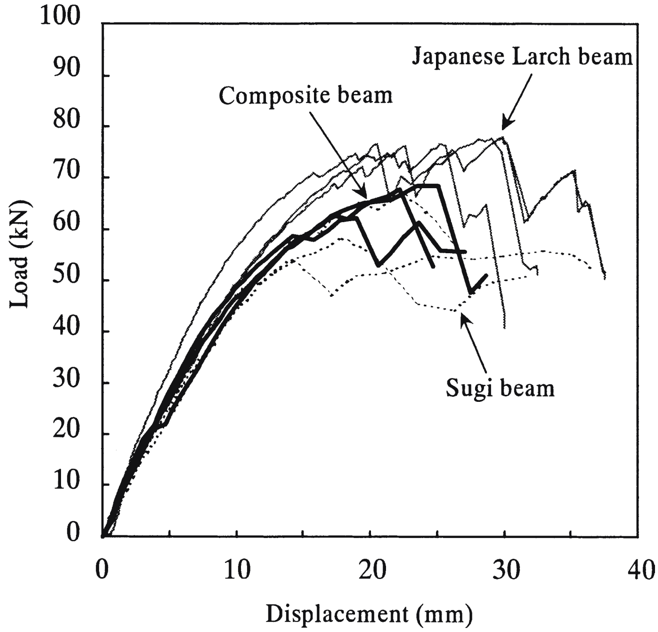

Fig. 10. Load–displacement curve (girder–beam specimens with 300 mm depth). Value used on displacement scale is the average of four readings obtained from displacement transducers

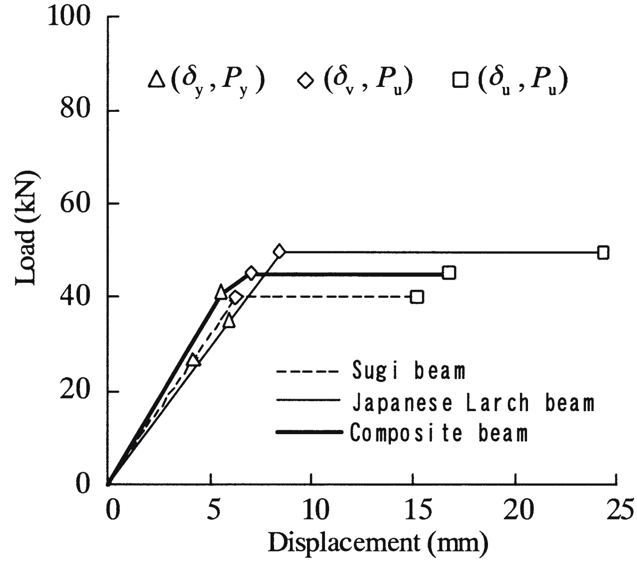

Fig. 11. Simplified and idealized load–displacement curves (post–beam specimens with 240 mm depth). For definitions of (δ_y, P_y), (δ_v, P_y), (δ_u, P_u), refer to Fig. 8

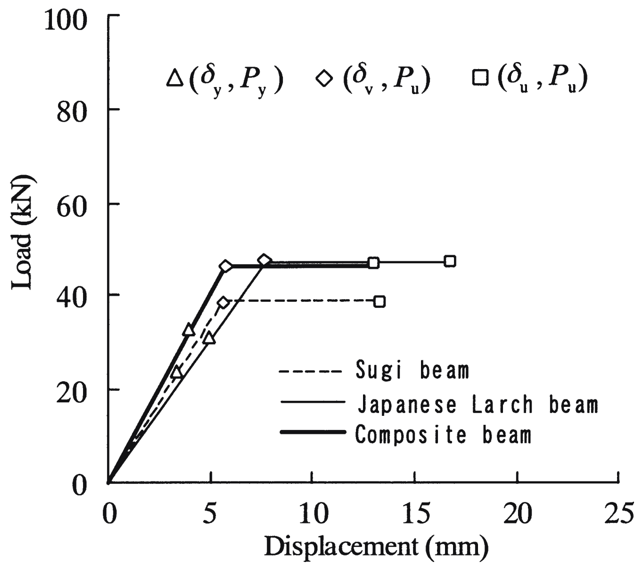

Fig. 12. Simplified and idealized load–displacement curves (girder–beam specimens with 240 mm depth)

Judging from the observation of the failure mode, the joints in the composite beams appeared to be stronger than those in the sugi beams, because splitting strength (mode I fracture energy) depends on the density of a lamina in which a drift pin hole is placed.

Load and displacement

Figure 10 shows some load–displacement curves for a girder beam specimen with a 300-mm depth. As is clear from Fig. 10, the relation between load and relative displacement of the joints is represented as a typical nonlinear curve. The same inclination is observed on load–displacement curves of other specimens.

Figures 11–14 show the simplified and idealized load–displacement curves of the joint. In these figures, (δ_y, P_y), (δ_v, P_u), and (δ_u, P_u) are the average of three sets of data obtained from three specimens. The simplified load–displacement curves of the joints in composite beam seem to be somewhere between those of sugi and Japanese larch beam.

Effects of variables

Tables 1 and 2 summarize the maximum load and initial stiffness of the joints, respectively. Each value is an average of three sets of data from three specimens. The percentage represents the ratio of each value relative to the corresponding sugi beam. Although there are several exceptions, it is generally found that the initial stiffness and maximum load of the joint in the composite beam were somewhere between those in sugi and Japanese larch beams.

The coordinates for the maximum load of joint in post–beam specimens and those in corresponding joints in girder–beam specimens are plotted in Fig. 15. As is clear from Fig. 15, most plots are located on the straight line, indicating that the maximum load of the joint is not influenced by the type of joint.

Table 3 summarizes the allowable loads of the joints. Almost all joints were evaluated with maximum load. Joints in composite beam showed higher allowable load than that in sugi beam, when the beam depth was 300 mm. On the other hand, the inclination was quite the opposite when the beam depth was 240 mm. This is because the joints in com-

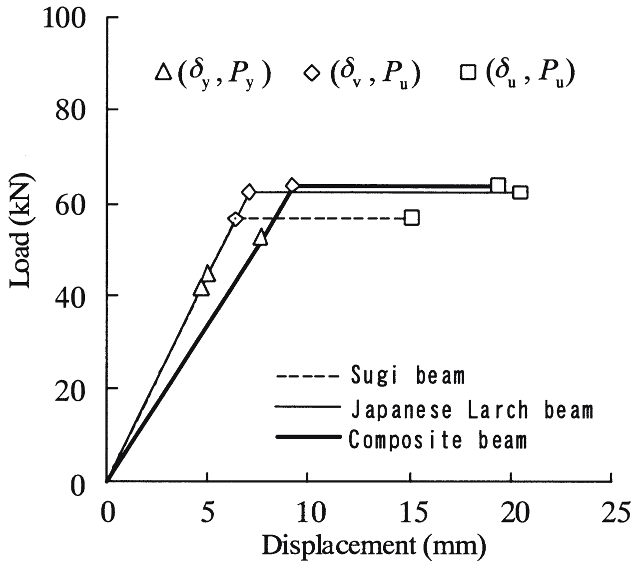

Fig. 13. Simplified and idealized load–displacement curves (post–beam specimens with 300 mm depth)

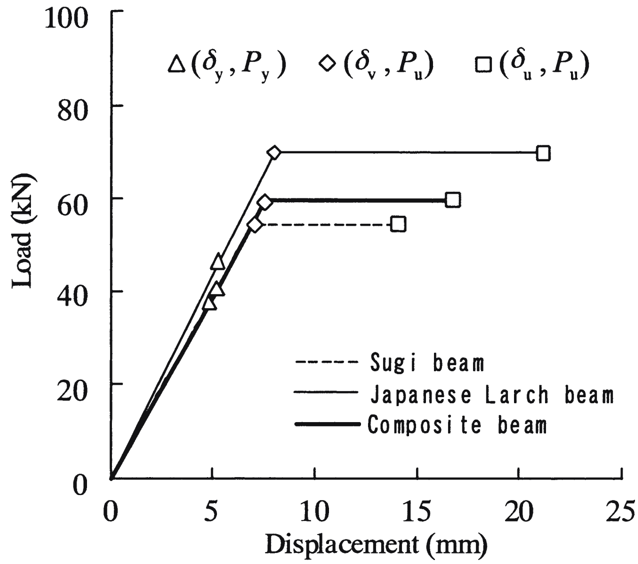

Fig. 14. Simplified and idealized load–displacement curves (girder–beam specimens with 300 mm depth)

Table 1. Maximum load of the tested joints

Type of joint	Beam depth (mm)		Type of beam		
			Sugi	Japanese larch	Composite
Gider–beam	240	No. 1	45.7	53.0	49.5
		No. 2	40.5	54.5	60.3
		No. 3	42.6	55.8	51.0
		Average	42.9 (100%)	54.4 (127%)	53.6 (125%)
		CV	0.06	0.03	0.11
	300	No. 1	59.5	76.8	69.4
		No. 2	67.3	78.0	67.8
		No. 3	56.3	77.9	63.0
		Average	61.0 (100%)	77.6 (127%)	66.7 (109%)
		CV	0.09	0.01	0.05
Post–beam	240	No. 1	48.8	55.8	45.6
		No. 2	42.5	55.4	49.7
		No. 3	46.3	56.9	56.8
		Average	45.9 (100%)	56.1 (122%)	50.7 (111%)
		CV	0.07	0.01	0.11
	300	No. 1	58.6	63.2	67.6
		No. 2	59.9	70.8	71.3
		No. 3	63.9	75.0	68.1
		Average	60.8 (100%)	69.7 (115%)	69.0 (113%)
		CV	0.05	0.09	0.03

Maximum load is for one connector. Results are in kN. Nos. 1,2,3 are the three specimens tested. Percentages represent the ratio of each value to that of the corresponding sugi specimen
CV, coefficient of variation

posite beam had larger variation of maximum load of joints than those in sugi beam (see Table 1).

Conclusions

The load–displacement curves of the joints in composite beam were somewhere between those in sugi and Japanese larch beam. The average shear strength of the joints in composite glulam beam was higher than that in sugi glulam beam. Thus, reinforcement of sugi glulam with Japanese larch lamination is apparently effective for improving the shear strength of the joint. However, the allowable load of joints in composite glulam was lower than that in sugi glulam beam with 240 mm depth because the joints in composite beam had large variation of maximum load of joints. Therefore, the test results presented here are not sufficient

Table 2. Initial stiffness of the tested joints

Type of joint	Beam depth (mm)		Type of beam		
			Sugi	Japanese larch	Composite
Gider–beam	240	No. 1	5.8	6.8	7.7
		No. 2	6.7	6.5	9.0
		No. 3	9.0	5.3	7.5
		Average	7.2 (100%)	6.2 (87%)	8.0 (112%)
		CV	0.24	0.13	0.10
	300	No. 1	8.0	7.4	6.9
		No. 2	7.0	10.9	8.3
		No. 3	8.5	8.7	8.9
		Average	7.9 (100%)	9.0 (114%)	8.0 (102%)
		CV	0.10	0.20	0.13
Post–beam	240	No. 1	6.0	5.5	4.1
		No. 2	5.8	5.4	9.7
		No. 3	7.6	7.0	8.3
		Average	6.5 (100%)	5.9 (92%)	7.4 (114%)
		CV	0.15	0.15	0.39
	300	No. 1	8.6	9.1	8.4
		No. 2	8.1	8.4	5.8
		No. 3	9.8	9.0	6.8
		Average	8.8 (100%)	8.8 (115%)	7.0 (79%)
		CV	0.10	0.04	0.19

Initial stiffness is for one connector. Results are in kN/mm. Nos. 1,2,3 are the three specimens tested. Percentages represent the ratio of each value to that of the corresponding sugi specimen

Table 3. Allowable load of the tested joints

Type of joint	Beam depth (mm)	Type of beam		
		Sugi	Japanese larch	Composite
Gider–beam	240	20.3 (100%)	31.9 (157%)	17.3 (85%)
	300	22.8 (100%)	49.6 (218%)	33.9 (149%)
Post–beam	240	20.7 (100%)	34.9 (169%)	15.9 (77%)
	300	31.9 (100%)	38.5 (121%)	39.7 (124%)

Results are in kN. Percentages represent the ratio of each value to that of the corresponding sugi specimen

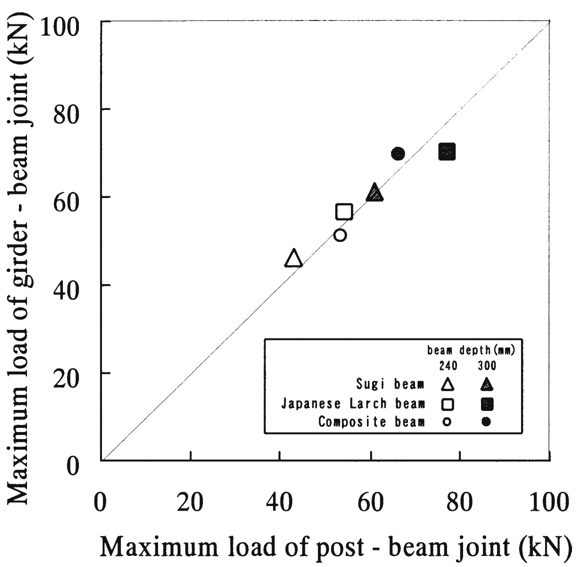

Fig. 15. Maximum loads of post–beam specimens compared with those of girder–beam specimens

to detect any significant difference in allowable load between joints in composite beams and sugi beams.

References

1. Hayashi T, Miyatake A (1991) Strength properties of Sugi composite glulam beams I (in Japanese). Mokuzai Gakkaishi 37: 200–205
2. Ministry of Agriculture, Forestry, and Fisheries (1996) Japanese agricultural standard for structural glued laminated timber. Japanese Agricultural Standards Association, Tokyo
3. Hayashi T, Karube M, Harada K, Mori T, Ohno T, Komatsu K, Iijima Y (2002) Shear tests of timber joints composed of Sugi composite glulam beams using newly developed steel connectors. J Wood Sci 48:484–490
4. Japan Housing and Wood Technology Center (2001) Design of the allowable load at wooden construction framework housing. Kogyo Chosakai, Tokyo